A Journal of the Gesellschaft Deutscher Chemiker

Angewandte International Edition Chemie

GDCh

www.angewandte.org

Accepted Article

Title: A De Novo Heterodimeric Due Ferri Protein Minimizes the Release of Reactive Intermediates in Dioxygen-dependent Oxidation

Authors: Marco Chino, Linda Leone, Ornella Maglio, Daniele D'Alonzo, Fabio Pirro, Vincenzo Pavone, Flavia Nastri, and Angela Lombardi

To be cited as: *Angew. Chem. Int. Ed.* 10.1002/anie.201707637
Angew. Chem. 10.1002/ange.201707637

Link to VoR: http://dx.doi.org/10.1002/anie.201707637
http://dx.doi.org/10.1002/ange.201707637

WILEY-VCH

10.1002/anie.201707637

WILEY-VCH

A *De Novo* Heterodimeric Due Ferri Protein Minimizes the Release of Reactive Intermediates in Dioxygen-dependent Oxidation

Marco Chino,[+] Linda Leone,[+] Ornella Maglio, Daniele D'Alonzo, Fabio Pirro, Vincenzo Pavone, Flavia Nastri, and Angela Lombardi*

Abstract: Metalloproteins utilize O_2 as an oxidant, and they often achieve a 4-electron reduction without H_2O_2 or oxygen radical release. Several proteins have been designed to catalyze one or two-electron oxidative chemistry, but the *de novo* design of a protein that catalyzes the net 4-electron reduction of O_2 has not been reported yet. We report here the construction of a diiron-binding four-helix bundle, made up of two different covalently linked α_2 monomers, through click chemistry. Surprisingly, the prototype protein, DF-C1, showed a large divergence in its reactivity from earlier DFs. DFs release the quinone imine and free H_2O_2 in the oxidation of 4-aminophenol in the presence of O_2, whereas Fe^{III}-DF-C1 sequesters the quinone imine into the active site, and catalyzes inside the scaffold an oxidative coupling between oxidized and reduced 4-aminophenol. The asymmetry of the scaffold allowed a fine-engineering of the substrate binding pocket, that ensures selectivity.

Nature accomplishes the activation of the highly stable dioxygen bond using different enzymes that often employ transition metal ions, such as copper or iron.[1-3] Metalloenzymes are spectacularly organized for processing O_2, and for catalyzing oxidation reactions of a variety of organic substrates with high selectivity, while avoiding diffusion of deleterious reactive intermediates.

Insights into structure-function relationships of natural dioxygen-activating metalloenzymes have partly derived from the study of biomimetic systems of different sizes and complexities.[4-6] The majority of these models uses highly reactive and unstable species as sacrificial oxidants (such as peroxides or peracids) rather than O_2.Progress in this field still represents a great challenge, for both mechanistic studies and practical applications.

Along these lines, we have developed the DF (Due Ferri, two-iron) family of *de novo* designed metalloproteins, to mimic the natural diiron-oxo-proteins.[7] The DF scaffold is made up by a stable four-helix bundle, able to tolerate several mutations for hosting different activities.[8-12] In particular, DF3 is an artificial phenol-oxidase that catalyzes the O_2-dependent oxidation of 4-aminophenol (4AP) to 4-benzoquinone monoimine (4BQM).[13,14] The released highly reactive product is rapidly quenched in solution by reaction with *m*-phenylendiamine (MPD) (Figure 1) to form the aminoindoaniline dye, spectrophotometrically detectable at 486 nm, pH 7.[15]

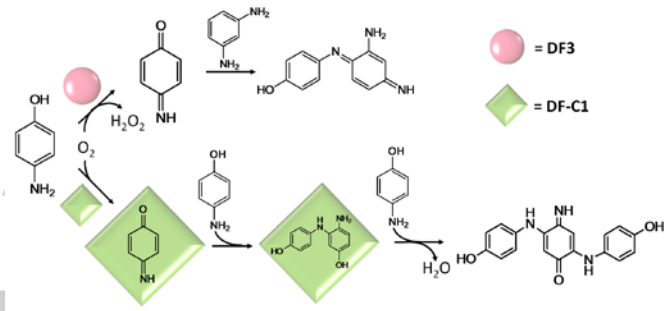

Figure 1. Reaction scheme depicting the O_2-dependent oxidation of 4AP catalyzed by Fe^{III}-DF3 (top) and Fe^{III}-DF-C1 (bottom). In the case of DF3, the oxidized 4BQM is released in solution and subsequently quenched with MPD. 4BQM is retained into the active site of DF-C1, where it undergoes coupling with another molecule of 4AP prior to be released.

The goal of the current work was to re-engineer the DF3 scaffold, in order to sequester the reactive quinoneimine intermediate inside the protein, to change the 4AP oxidation pathway. We targeted toluene mono-oxygenase proteins (TMOs)[16,17] and tried to transplant the asymmetry of their active site into DF3. Using a design method, recently developed by us,[18] we obtained an asymmetric four-helix bundle (DF-C1) through click chemistry,[19] a strategy rarely used in protein design.[20,21] We chose the Cu^I catalyzed azide-alkyne cycloaddition (CuAAC)[22] to selectively link two different α-helical hairpins. To this aim, we inserted propargyl glycine (Pra) and 6-azido-hexanoic acid (6-aha) into the DF3 sequence (Figure 2a), leading to two *clickable* chains (K and Z, respectively). Pra and 6-aha positions in each chain were evaluated by computational screening,[18] based on the NMR structure of DF3 (PDB 2KIK)[13] (Figure S1).

Beside the clicking residues, we introduced into the DF3 sequence a total of nine mutations, which can be categorized into three classes, intended to: *i)* modulate active site access, substrate recognition and catalysis; *ii)* form H-bond network; *iii)* improve packing (Figures 2b, S2, S3, Supporting Information). We first considered that four Gly lined the active site cavity in DF3, creating a wide access channel; this was made narrower and more hydrophobic in DF-C1, by mutating $G13_KT$ and $G9_ZF$ (subscript K or Z indicates the chain). Remarkably, these two mutations play additional roles: $G9_ZF$, together with $Y17_ZL$ and $Y17_KF$, mimic the Phe-rich pocket found in TMOs;[23] $Y17_ZL$ mutation also prevents the off-pathway tyrosinate-iron complex

[*] Dr. M. Chino, Dr. L. Leone, Dr. D. D'Alonzo, Dr. F. Pirro, Prof. V. Pavone, Prof. F. Nastri, Prof. A. Lombardi
Department of Chemical Sciences
University of Napoli "Federico II"
Via Cintia, 80126 Napoli (Italy)
E-mail: angela.lombardi@unina.it
Dr. O. Maglio
IBB - National Research Council
Via Mezzocannone 16, 80134 Napoli (Italy)
[+] These authors contributed equally to this work
Supporting Information for this article is given via a link at the end of the document.

formation, previously reported by Reig et al.;[10] $G13_KT$, together with $L33_KQ$, could stabilize a water molecule involved in proton transfer.[24,25]

Next, a new second-shell H-bond was introduced by $L43_KN$ mutation, which, together with $L29_ZQ$ mutation, enabled the formation of an H-bond network comprising $E10_K$-$N43_K$-$Q29_Z$-$N26_Z$ (Figure 2b). Finally, two additional mutations were inserted to optimize packing ($Q16_KL$, $I14_KA$).

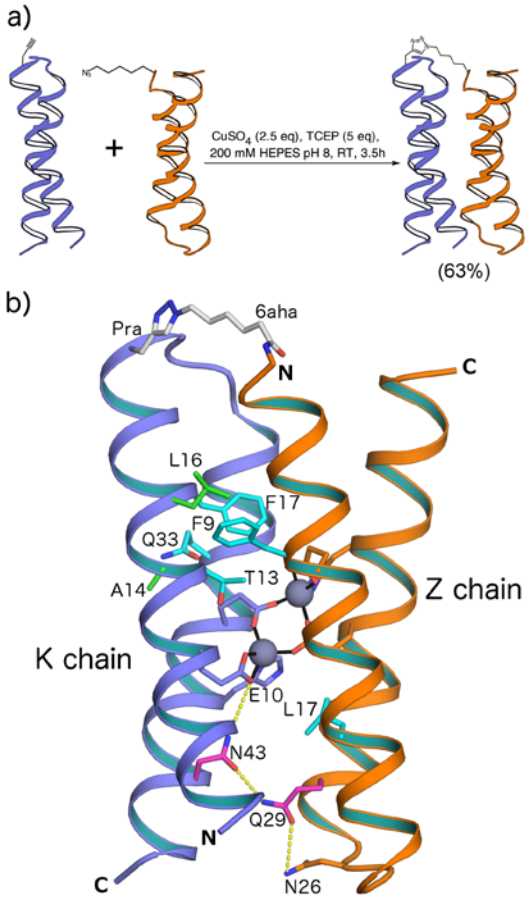

Figure 2. a) DF-C1 click reaction scheme; K- and Z-chains are in blue and orange, respectively. b) Energy minimized model of Zn^{II}-DF-C1. All the mutated residues respect to DF3 are in sticks. The three classes of mutations are highlighted in different colors: *i)* active site access substrate recognition and catalysis (cyan); *ii)* H-bond network (magenta); *iii)* packing improvement (green). The hydrogen bond network, spanning from E10(K) to N26(Z), is reported as dashed yellow lines.

The synthetic K and Z chains were coupled through CuAAC in buffered solution at pH 8.0 (Figures 2a, S4-S7, Supporting Information).

Spectroscopic characterization by CD, UV/Vis and NMR indicated that DF-C1 binds two metal ions *per* protein, within a well-folded structure.

The CD spectrum of the *apo*-protein at pH 7.0 is typical of a α-helical structure (Figure S8). Addition of Fe^{II} (Figure 3a) (as well as Zn^{II} and Co^{II}, Figure S9) to *apo*-DF-C1 led to an increase in the ellipticity at 208 and 222 nm, indicating a further increase in the helical content. CD titrations indicated a reasonably tight binding, with the expected 2:1 metal:protein stoichiometry (Figures 3b and S9).

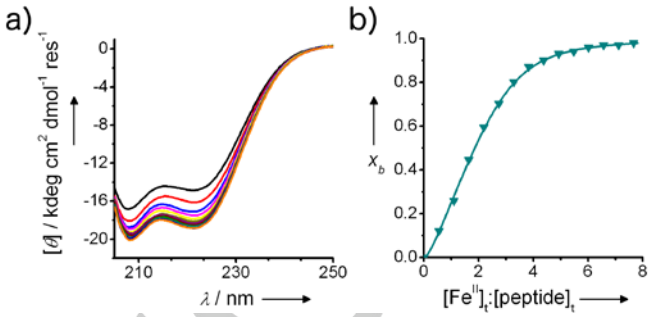

Figure 3. Folding and Fe^{II}-binding analyses of DF-C1.a) CD spectral changes upon Fe^{II} addition. b) CD titration curve of *apo*-DF-C1 with Fe^{II}. The fraction bound (x_b) is plotted *versus* Fe^{II} equivalents. The smooth curve represents the best fit for a binding isotherm with a 2:1 (Fe^{II}:Peptide) stoichiometry, and pK_{diss} 5.61 ± 0.03 (R^2 = 0.996; see Supporting Information).

Insight into the coordination geometry was obtained from the absorption spectrum of the Co^{II} complex (Supporting Information). Position and intensities of the bands (Figure S10) are indicative of either *bis*-five coordinate or five/six coordinate geometry,[26] as typically observed in Co^{II}-reconstituted diiron proteins (Table S1).[27]

Finally, the NMR spectrum of the diamagnetic Zn^{II}-complex exhibits features of a well-folded protein, with narrow line-widths and well-dispersed proton chemical shifts, in both the amide and aliphatic regions (Figure S11). Furthermore, Diffusion-Ordered NMR spectroscopy (DOSY) gave a hydrodynamic radius (R_H) value of 24±2 Å, comparable to that calculated for the model (23.4 Å) (Figure S12), confirming the intended folded state.[28,29]

Fe^{II}-DF-C1 reacts with O_2 to form the oxo-bridged diferric species, as monitored by the appearance of the ligand-to-metal-charge transfer (LMCT) band at 350 nm (ε: 5500 $M^{-1}cm^{-1}$, as expected for this class of proteins, see Figure S13 and Table S2).[14]

To test whether the active site re-design was successful in driving a different reaction pathway respect to Fe^{III}-DF3, we investigated the reactivity of Fe^{III}-DF-C1in the oxidation of 4AP. Differently from DF3, no significant formation of the aminoindoaniline dye was observed when the 4AP oxidation was performed in the presence of MPD (data not shown). The addition of sole 4AP to a solution of Fe^{III}-DF-C1, in the presence of ambient O_2, led to the formation of two absorption bands at 370 nm and 470 nm, whose intensities increased over time (Figure 4a).

The corresponding reaction with Fe^{III}-DF3 revealed a different spectroscopic behavior, with the appearance of two bands at 370 nm and 500 nm (Figure 4b). Both bands achieved their maximum intensities within 1 h, and subsequently, their intensities decreased over several hours, with the concomitant formation of a brownish precipitate.

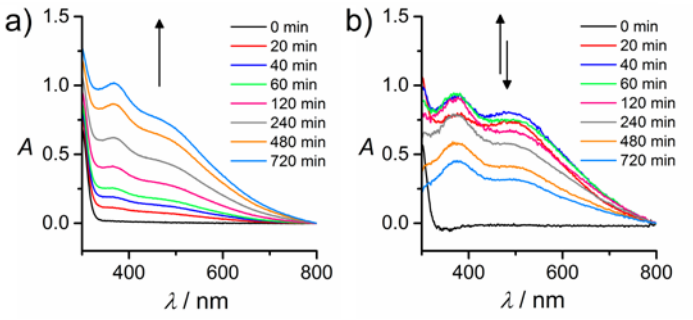

Figure 4. UV/Vis spectra of the oxidation of 4AP by: a) Fe^{III}-DF-C1; b) Fe^{III}-DF3. Fe^{III}-DF3 begun giving product precipitation after 1 h. Experimental conditions: 40 μM catalyst, 400 μM 4AP; 10 mM HEPES, 10 mM Na_2SO_4 pH 7)

To identify the compounds formed in the reactions catalyzed by the two enzymes, the mixtures were analyzed by HPLC, 1 hour after mixing (Figure 5). A single peak, at r_t=15 min, was observed in the chromatogram, when Fe^{III}-DF-C1 was used as catalyst (Figures S15, S16). The product was identified as the oxidation/condensation derivative of 4AP (Figure 5, **1**, Figure S17, Table S4), analog of the Bandrowski's base.[30] The HPLC profile of 4AP oxidation, catalyzed by Fe^{III}-DF3, revealed instead the formation of multiple products, with compound **1** representing only a minor component (≈ 20% of total yield; Figure 5, S18). A control reaction, carried out using stoichiometric amount of Fe^{II} ammonium sulfate, revealed no product formation (Figures S20, S21).

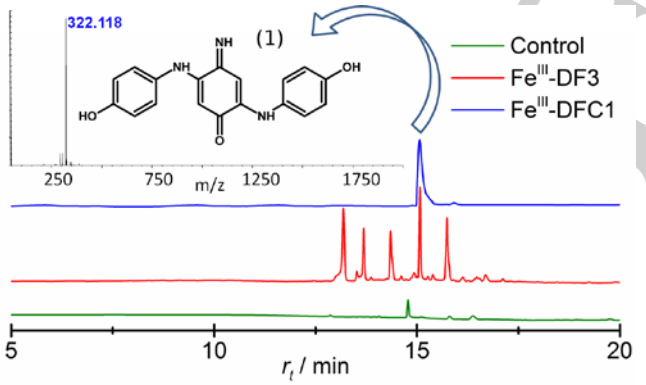

Figure 5. HPLC traces at 254 nm of 4AP oxidation in presence of: Fe^{III}-DF-C1 (blue), Fe^{III}-DF3 (red), Fe^{II} ammonium sulfate (green). All traces were acquired after 1 hour of reaction progress. Peak eluted at 15 min has been identified as compound **1**. Inset: ESI-IT-TOF mass spectrum of compound **1**.

These results provide evidence that Fe^{III}-DF3 is an "imperfect" catalyst, respect to Fe^{III}-DF-C1, in the 4AP oxidation, being uncontrolled and thereby less selective. This allowed us to propose different reaction pathways for the two catalysts. 4AP is oxidized at the diiron site of DF3 with release of the reactive 4BQM and free H_2O_2 in solution (Figure 1). In the absence of MPD, 4BQM spontaneously couples in solution with 4AP, to give compound **1**, with the rate-limiting step being the first coupling reaction.[30] Formation of additional by-products (Figure 5) could derive from H_2O_2-dependent degradation of compound **1**, 4BQM or the other reaction intermediates. Upon addition of catalase (200 U/mL) to remove the diffusing H_2O_2, Fe^{III}-DF3 produced only **1**, similarly to Fe^{III}-DF-C1 (Figures S22).

Differently from Fe^{III}-DF3, Fe^{III}-DF-C1 prevents the diffusion in solution of the reactive 4BQM intermediate (Figure 6).The designed second-shell interactions would favor 4AP oxidative dimerization coupled to O_2 reduction in two successive two-electron steps inside the protein. The 4AP would thus be kept tightly bound into the protein scaffold after being oxidized to 4BQM, leading to dimer formation (oxidation), with *in situ* peroxide consumption.

In this scenario, the rate-limiting step would be the release of the oxidized dimer in solution, which in turns, by coupling with another equivalent of 4AP, affords **1** (Figure 6).

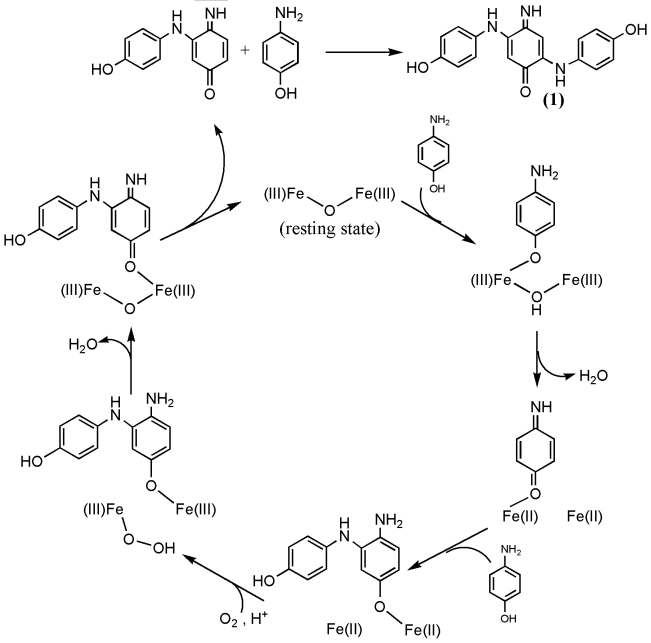

Figure 6. Proposed catalytic cycle for the Fe^{III}-DF-C1catalyzed 4AP oxidation.

The proposed mechanism is supported by the following evidences. Firstly, catalase or superoxide dismutase addition does not cause any change in the product identity (Figure S23). Moreover, no product formation was observed upon addition of different substrates and hydrogen peroxide to Fe^{III}-DF-C1, thus ruling out the involvement of peroxide in the mechanism (see Supporting Information).

Secondly, addition of one equivalent of 4AP to Fe^{III}-DF-C1, under aerobic conditions, caused the appearance of a broad band around 500 nm (Figure S24a). These spectral changes suggest that 4AP binds to the diferric center, giving rise to a ligand to metal charge-transfer transition.[9,31] Further, addition of 10 eq. of 4AP under anaerobic conditions led to the reduction of the di-ferric to the diferrous center, as ascertained by the decrease of the band at 350 nm (Figure S24b). Upon dioxygen addition, formation of compound **1** was observed.

Finally, analysis of the docking model between the 4AP dimer and DF-C1 revealed that 4AP dimer properly fits into the designed pocket, suggesting a key role of the designed Phe9 in guiding the dimer formation by π-stacking interaction (Figure S25a and S26). Interestingly, when 4AP dimer was docked to DF3, no specificity was observed in the wider binding pocket (Table S6 and Figure S25b), suggesting the intrinsically lower driving force for the 4AP coupling to take place. Further mechanistic studies are however required to carve out completely all the intermediates involved in the reaction pathway. This will lead to a deeper understanding of the mechanism herein hypothesized, and eventually will open to unconsidered alternatives.

In conclusion, we successfully applied a new method to modify the DF3 scaffold and generate the asymmetricDF-C1, by covalent ligation of two functionalized α_2 peptides through click chemistry. This approach, never used before for the design of four helix bundle proteins, allowed us to engineer carefully the second-shell active site interactions and to sequester a reactive intermediate inside the protein. With this in hand, we succeeded in steering the reaction mechanism and product distribution of a di-iron protein. The present study shows that in 4AP oxidation the diiron site performs four-electron O_2 reduction in two successive two-electron steps inside the protein. This finding fills the gap between *de novo* designed and natural proteins.[32] The efficiency of the new catalyst is still far from natural oxidases and oxygenases; however, the asymmetry of the scaffold, and the boost offered by the synthetic method will allow for a fine-tuning of the active site steric and electronic properties, thus affecting the overall reactivity and specificity.

Acknowledgements

The authors thank W.F. DeGrado for helpful suggestions and Fabrizia Sibillo for technical assistance. The Cost Action CM1003 and the Scientific Research Department of Campania Region (STRAIN Project, grant number B25B0900000000, postdoctoral fellowship to M.C.) are also acknowledged.

Keywords:bioinorganic chemistry•*de novo* protein design•oxidoreductase•diiron-oxo proteins•click chemistry

[1] A. Decker, E. I. Solomon, *Curr. Opin. Chem. Biol.* **2005**, *9*, 152.
[2] S. Sahu, D. P. Goldberg, *J. Am. Chem. Soc.* **2016**, *138*, 11410.
[3] M. V. Doble, A. C. C. Ward, P. J. Deuss, A. G. Jarvis, P. C. J. Kamer, *Bioorg. Med. Chem.* **2014**, *22*, 5657.
[4] F. Nastri, M. Chino, O. Maglio, A. Bhagi-Damodaran, Y. Lu, A. Lombardi, *Chem. Soc. Rev.* **2016**, *45*, 520.
[5] Y. Lin, *Coord. Chem. Rev.* **2017**, *366*, 1.
[6] L. A. Churchfield, A. George, F. A. Tezcan, *Essays Biochem.* **2017**, *61*, 245.
[7] M. Chino, O. Maglio, F. Nastri, V. Pavone, W. F. DeGrado, A. Lombardi, *Eur. J. Inorg. Chem.***2015**, *2015*, 3371.
[8] S. Geremia, L. Di Costanzo, L. Randaccio, D. E. Engel, A. Lombardi, F. Nastri, W. F. DeGrado, *J. Am. Chem. Soc.* **2005**, *127*, 17266.
[9] J. Kaplan, W. F. DeGrado, *Proc. Natl. Acad. Sci. USA* **2004**, *101*, 11566.
[10] A. J. Reig, *et al.*, *Nat. Chem.* **2012**, *4*, 900.
[11] R. A. Snyder, S. E. Butch, A. J. Reig, W. F. DeGrado, E. I. Solomon, *J. Am. Chem. Soc.* **2015**, *137*, 9302.
[12] R. A. Snyder, J. Betzu, S. E. Butch, A. J. Reig, W. F. DeGrado, E. I. Solomon, *Biochemistry* **2015**, *54*, 4637.
[13] M. Faiella, C. Andreozzi, R. Torres Martin de Rosales, V. Pavone, O. Maglio, F. Nastri, W. F. DeGrado, A. Lombardi, *Nat. Chem. Biol* .**2009**, *5*, 882.
[14] R. Torres Martin de Rosales, M. Faiella, E. Farquhar, L. Que, C. Andreozzi, V. Pavone, O. Maglio, F. Nastri, A. Lombardi, *J. Biol. Inorg. Chem.* **2010**, *15*, 717.
[15] J. F. Corbett, *J. Chem. Soc. B Phys. Org.* **1969**, 823.
[16] M. S. McCormick, M. H. Sazinsky, K. L. Condon, S. J. Lippard, *J. Am. Chem. Soc.* **2006**, *128*, 15108.
[17] L. J. Bailey, B. G. Fox, *Biochemistry* **2009**, *48*, 8932.
[18] M. Chino, L. Leone, O. Maglio, A. Lombardi, *MethodsEnzymol.* **2016**, *580,* 471.
[19] H. C. Kolb, M. G. Finn, K. B. Sharpless, *Angew. Chem. Int. Ed.* **2001**, *40*, 2004; *Angew. Chem.* **2001**, *113*, 2056.
[20] W. S.Horne, M. K. Yadav, C. D. Stout, M. R. Ghadiri, *J. Am. Chem. Soc.* **2004**, *126*, 15366.
[21] J. M. Beierle, W. S. Horne, J. H. van Maarseveen, B. Waser, J. C. Reubi, M. R. Ghadiri, *Angew. Chem. Int. Ed.* **2009**, *48,* 4725; *Angew. Chem.* ***2009***, *121*, 4819.
[22] V. D. Bock, H. Hiemstra, J. H. van Maarseveen, *Eur. J. Org. Chem.* **2006**, *2006*, 51.
[23] M. H. Sazinsky, J. Bard, A. Di Donato, S. J. Lippard, *J. Biol. Chem.* **2004**, *279*, 30600.
[24] N. L. Elsen, L. J. Bailey, A. D. Hauser, B. G. Fox, *Biochemistry* **2009**, *48*, 3838.
[25] W. J. Song, M. S. McCormick, R. K. Behan, M. H. Sazinsky, W. Jiang, J. Lin, C. Krebs, S. J. Lippard, *J. Am. Chem. Soc.* **2010**, *132*, 13582.
[26] I. Bertini, C. Luchinat, *Adv. Inorg. Biochem.* **1984**, *6*, 71.
[27] M. H. Sazinsky, M. Merkx, E. Cadieux, S. Tang, S. J. Lippard, *Biochemistry* **2004**, *43*, 16263.
[28] J. A. Jones, D. K. Wilkins, L. J. Smith, C. M. Dobson, *J. Biomol. NMR* **1997**, *10*, 199.
[29] J. García de la Torre, M. L. Huertas, B. Carrasco, *J. Magn. Reson.***2000**, *147*, 138.
[30] J. F. Corbett, E. P. Gamson, *J. Chem. Soc. Perkin Trans. 2* **1972**, 1531.
[31] J. R. Calhoun, C. B. Bell, T. J. Smith, T. J. Thamann, W. F. DeGrado, E. I. Solomon, *J. Am. Chem. Soc.* **2008**, *130*, 9188.
[32] F. Yu, V. M. Cangelosi, M. L. Zastrow, M. Tegoni, J. S. Plegaria, A. G. Tebo, C. S. Mocny, L. Ruckthong, H. Qayyumand, V. L. Pecoraro, *Chem. Rev.* **2014**, *114*, 3495.

10.1002/anie.201707637

WILEY-VCH

Table of Contents

COMMUNICATION

Not just a four helix bundle: The use of four helix bundle scaffold with an asymmetric active site leads to an enhancement in selectivity of the iron-catalyzed oxidative coupling of phenols. The stabilization of the oxidized intermediate in the engineered binding pocket enables the net four-electron O_2 reduction, without release of any detectable H_2O_2. The newly engineered activity is unprecedented for this family of catalysts.

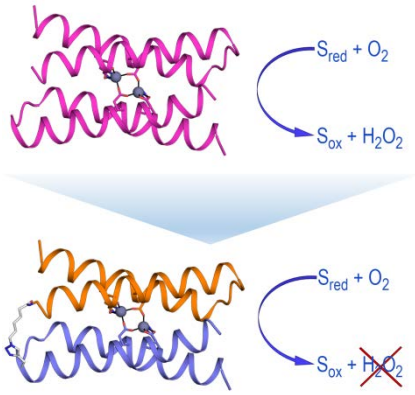

*Marco Chino, Linda Leone, Ornella Maglio, Daniele D'Alonzo, Fabio Pirro, Vincenzo Pavone, Flavia Nastri, Angela Lombardi**